

UC Berkeley

UC Berkeley Previously Published Works

Title

Mapping the Transmission Functions of Single-Molecule Junctions

Permalink

<https://escholarship.org/uc/item/9z57s9z6>

Journal

Nano Letters, 16(6)

ISSN

1530-6984

Authors

Capozzi, Brian
Low, Jonathan Z
Xia, Jianlong
[et al.](#)

Publication Date

2016-06-08

DOI

10.1021/acs.nanolett.6b01592

Peer reviewed

Mapping the Transmission Function of Single-Molecule Junctions

Brian Capozzi¹, Jonathan Z. Low², Jianlong Xia², Zhen-Fei Liu³, Jeffrey B. Neaton^{3,4}, Luis M. Campos², Latha Venkataraman^{1,2}

¹Department of Applied Physics and Applied Mathematics, and

²Department of Chemistry, Columbia University, New York, NY 10027

³Molecular Foundry, Lawrence Berkeley National Laboratory,

⁴Department of Physics and Kavli Energy Nano Sciences Institute, Berkeley, CA 94720

ABSTRACT

Charge transport characteristics of single-molecule junctions are often governed by a transmission function that dictates the probability of electrons or holes tunneling across the junction. Here, we present a new and simple technique for measuring the transmission function of molecular junctions in the coherent tunneling limit, over an energy range of 2 eV around the Fermi energy. We create molecular junctions in an ionic environment with electrodes having different areas exposed, which results in the formation of electric double layers of dissimilar density on the two electrodes. This allows us to electrostatically shift the molecular resonance relative to the junction Fermi levels in a manner that depends on the sign of the applied bias, enabling us to map out the junction's transmission function and determine the dominant orbital for charge transport in the molecular junction. We demonstrate this technique using two groups of molecules: one group having molecular resonance energies relatively far from E_F and one group having molecular resonance energies within the accessible bias window. Our results compare well with previous electrochemical gating data and with transmission functions computed *ab initio*. Furthermore, with the second group of molecules, we are able to examine the behavior of a molecular junction as a resonance shifts into the bias window. This work provides a new, experimentally simple route for exploring the fundamentals of charge transport at the nanoscale.

Characterizing metal-molecule interfaces is a key step in developing organic electronic devices, as interfacial properties serve to dictate device properties. One of the most fundamental “interfaces” in organic electronics is the single metal-molecule bond: this interface can be readily created and studied using break junction techniques.^{1,2} Advances in the study of single-molecule circuits have led to a wealth of knowledge regarding the electronic and mechanical properties of such systems, as well as the mechanisms by which charge is transported.^{3,4} For many systems investigated thus far, charge transport occurs via coherent tunneling, and can therefore be described by a transmission function detailing the energy-dependent probability that an incident electron or hole tunnels through the barrier presented by the junction.⁵

Several techniques have emerged to experimentally assess energy-level alignment at the metal-molecule interface in single-molecule junctions, including thermopower measurements⁶⁻⁸, alternating current (AC) techniques⁹, mapping of current-voltage curves¹⁰, and gating.¹¹ However, these methods have been unable to provide a detailed map of the transmission landscape, and have instead only provided limited insight into the transmission function. For example, thermopower measurements⁶ only give access to two quantities: low-bias conductance and the Seebeck coefficient. These can then be related to the value of the transmission function at E_F and its slope.¹² Using a recently developed AC method, currents can be measured at the first and second harmonics of an applied AC voltage (this AC modulation is on top of a direct current [DC] voltage); these values correspond to the first and second derivatives of the transmission function.⁹ These two methods, however, provide transmission function data at only two points; extracting further details of the level alignment requires assuming a functional form for transmission, commonly a two-parameter single-Lorentzian, and solving for the parameters. These methods therefore fail in junctions where a single-Lorentzian approximation for transmission is not valid.^{13,14}

Current-voltage (IV) curves can, in principle, be fit in order to obtain the transmission function since the measured current at a given voltage is proportional to an integral of the transmission function.¹⁰ However, such fitting requires knowledge of how the bias drops across the junction – and how the bias window opens about the average junction Fermi level – in addition to knowing the functional form for transmission. Furthermore, these fitting procedures are valid only if high-bias effects (such as stark shifted molecular levels¹⁵) can be excluded. Using a gate to electrostatically tune energy level alignment in the molecular junction (by

shifting molecular orbital energies relative to the electrode E_F) should provide the most direct experimental access to the transmission function. Unfortunately, gating techniques have proven difficult to implement at the single molecule level. Indeed, back- and side- gated devices require extensive fabrication processes and have typically had very low yields of working devices.¹⁶ Electrolyte gating alleviates the problem of needing to place a gate electrode in close proximity of the molecular junction.¹⁷ In principle, though, this technique then requires two additional electrodes in solution, a reference electrode and a counter electrode, which need to be controlled using a bipotentiostat, posing challenges to extending this technique to other electrode materials or device architectures.

Here, we report the development of a simple method that can be used to probe transmission in single-molecule junctions over an energy range of about 2 eV. Taking advantage of an asymmetric environment created by carrying out transport measurements in an ionic medium with electrodes of considerably different exposed areas, we are able to map the transmission function by simply performing conductance measurements over a range of source-drain biases.¹⁸ This removes the complication of needing additional electrodes and provides information about the transmission function without requiring knowledge of its functional form. We demonstrate this technique using different classes of molecular junctions, ones with resonances far from E_F and ones accessible within the bias window. In the latter case, we find that as the bias window approaches the resonance energy for one thiophene-dioxide derivative, the junctions rupture; while for an ethylenedioxythiophene derivative, we are able to open the bias window through the molecular resonance. Interestingly, we measure a decrease in current as the molecular orbital resonance enters the bias window, implying that the line-shape of the transmission function is changed by the bias. We hypothesize that this may occur due to a change in the coupling between the molecule and the electrode as the molecular orbital is charged and present a simple model to understand this effect.

Results and Discussion

We study charge transport in single-molecule junctions using the scanning tunneling microscope-based break junction (STM-BJ) technique.^{2, 19} Break junction measurements are carried out in a polar solvent (propylene carbonate, PC) using a gold tip insulated with Apiezon²⁰ wax in order to reduce any background electrochemical currents (schematic, Figure 1a). Conductance measurements are then performed by repeatedly driving the tip into and out of

contact with the substrate; upon retracting the tip, the gold junction is thinned down to a single-atom contact, which subsequently ruptures and yields a sub-nanometer gap between two atomically sharp electrodes. When this process is repeated in the presence of molecules that are terminated with gold-binding groups, a single-molecule can bridge the gap and the conductance of the metal-molecule-metal junction is measured. We first measure the conductance of 4,4'-bipyridine (**1**) and 4,4''-*p*-diaminoterphenyl (**2**) under these conditions. Measurements are compiled into logarithmically binned conductance histograms, which show peaks at molecule specific values. In Figure 1b, we show two histograms for **1** obtained when the tip is biased at +0.5V and -0.5V relative to the substrate. In both histograms, two conductance peaks are seen; these have been attributed to two distinct binding geometries for the molecule. The lower conductance (LG) corresponds to a fully elongated junction where the molecule is bound vertically between the Au electrodes through Au-N donor-acceptor bonds.²¹ The higher conductance (HG) corresponds to a tilted junction where there is an additional pi-coupling between the pyridine rings and the Au electrodes.^{21, 22} For both junction geometries, there is a clear dependence of the conductance peak position on the bias polarity, with a higher conductance observed at a negative bias. Such a bias polarity-dependent conductance is only observed in the polar solvent. Measurements performed in 1-octylbenzene at +/-0.5V show no shift in the conductance peaks (see inset of Figure 1b). In Figure 1c, we show conductance histograms for **2** measured at +/- 0.5 V. We again see a clear shift in the conductance histogram peaks with bias polarity. We note that the conductance histogram for molecule **2** at +0.5 V in PC also displays a distinct double peak feature. Here, we attribute the second peak to a junction with two molecules in parallel as the higher conductance is almost exactly twice the lower one. Conductance histograms in PC are significantly narrower than their 1-octylbenzene counterparts, enabling the multi-molecule junctions to be resolved more clearly. For both one- and two-molecule junctions, the measured conductance is higher when the tip is biased positively relative to the substrate. Interestingly, the formation rate of two-molecule junctions (and indeed even of one molecule junctions) is greatly diminished at -0.5V. Again, this in contrast to measurements performed in 1-octylbenzene (inset Fig. 1c), which do not show any dependence on bias polarity.

These results are in accord with our previous work¹⁸ where we have shown that the conductance of a molecular junction, even one containing a symmetric molecule, in an ionic environment with electrodes of considerably different exposed areas is dependent on both the

magnitude and polarity of the applied bias.¹⁸ This occurs because of the formation of double layers at the solution/electrode interfaces.²³ The disparity in areas of the two electrodes yields a much denser double layer at the tip, which is partially coated with wax and has a much smaller area exposed to the solvent. This dense double layer leads to a bias polarity-dependent shift of the molecular junction resonance energy, resulting in rectification. Considering the expression for current within the Landauer model, and assuming coherent tunneling through the junction and zero temperature, we have,²⁴

$$I = \frac{2e}{h} \int_{-eV/2}^{eV/2} T(E) dE \quad , \quad (1)$$

where $T(E)$ is the energy-dependent transmission function, V is the bias voltage, e is the charge on the electron and h is Planck's constant. The bias-dependent environmental asymmetry can then be modeled by incorporating a parameter, α , describing the shift in the transmission function with respect to the junction Fermi energy due to the applied voltage similar to that of a first-order Stark shift coefficient. Effectively, the α parameter describes how transmission resonances shift relative to the average junction Fermi level: if the resonances do not shift, $\alpha=0$; if the resonance is pinned to one electrode, $\alpha=0.5$. With the strong asymmetry in the double layer density (due to the large area mismatch between the tip and substrate), we have previously shown experimentally that $\alpha=0.5$ in our measurements.¹⁸ Within this picture, when the tip is biased negatively relative to the substrate, the resonances associated with the molecular orbitals shift down relative to average junction Fermi level, μ_F ; that is, the lowest unoccupied molecular orbital (LUMO) resonance shifts further into the bias window and closer to μ_F , and the highest occupied molecular orbital (HOMO) resonance shifts away from μ_F . When the tip is biased positively relative to the substrate, the reverse is true and the LUMO moves away from μ_F while HOMO nears μ_F . We thus expect the conductance of a LUMO-dominated molecule, to increase with increasingly negative tip biases, as we observe for **1**, while we would expect the conductance of a HOMO-dominated molecule to increase with increasingly positive tip biases, as we observe for **2**.

We now extract transmission function values for junctions with molecules **1** and **2** by performing conductance measurements in intervals of 100 mV. To obtain these transmission function values from the conductance data, we make a change of variable (from E to $E'=E+eV/2$) and using $\alpha = 0.5$, equation (1) can be expressed as,

$$I = \frac{2e}{h} \int_0^{eV} T(E' - eV/2) dE' \quad . \quad (2)$$

Physically, the bias window is still opening symmetrically around E_F however, the reformulation of equation 2 allows for the straightforward extraction of transmission function for a molecular junction. We assume here that the transmission function is unchanged with applied bias, (however, as we will show later in this article, this need not be true when the bias window approaches the resonance). By performing measurements at regular intervals we can determine the current, and hence the transmission probability, for sufficiently small energy interval along the transmission function:

$$G(V_2) - G(V_1) \approx T\left(\frac{E_2 + E_1}{2}\right) \cdot (V_2 - V_1) \quad . \quad (3)$$

We perform conductance measurements for **1** and **2** at tip bias voltages in intervals of 100mV (from -700mV to 500mV for **1** and from -500mV to 700mV for **2**, see conductance histograms in the Supplementary Information, SI). We plot the peak conductance values versus applied voltage for the two molecules in the insets of Figures 2a and 2b. Negative biases yield higher conductance values for **1** while positive biases yields higher conductance values for **2**. The extracted transmission values are then shown as insets in Figures 2a and 2b.

We compare our extracted transmission values with transmission functions previously calculated with the DFT+ Σ approach.¹¹ In Figure 2c, we overlay our transmission values with calculated transmission functions for both HG and LG geometries of molecule **1**, from Kim et al,⁸ and find that there is good agreement between the predicted and measured transmission. For this system, it is also possible to approximate $T(E)$ with a single Lorentzian in an energy range around the bias window. The Lorentzian parameters obtained from fits to our experiments are also in good agreement with the values obtained from other methods (see SI for details). In Figure 2d, we overlay a calculated transmission function from previous work⁸ for molecule **2**; we again find excellent agreement between the measured transmission and the ab initio prediction. For two-molecule junctions, we divide the measured transmission values by 2 (accounting for two molecules in parallel, and assuming no cooperative effects)²⁵, and overlay these values on the computed one-molecule transmission function. Again, we find good agreement between our measurements and the calculations. We also note that for molecule **2**, $T(E)$ cannot be

approximated using a single Lorentzian because of the presence of Au d-states at around -1.8 eV.⁸

Next, we can examine junctions that have resonances located substantially closer to E_F than those with molecules **1** and **2**. For this, we turn to transport measurements on two thiophene-derivative containing oligomers that have a small HOMO-LUMO-gap. Molecule **3** is composed of four electron deficient thiophene dioxide (TDO) units flanked on either side by methyl-sulfide bearing thiophenes; molecule **4** consists of a electron rich unit, 3,4-ethylenedioxythiophene (EDOT), flanked by two thiophenes with the terminal thiophenes containing the gold-binding methyl sulfides (see structures in Figures 3a and b). TDO units are used for lowering the energy of the LUMO²⁶ and EDOT to raise the HOMO.²⁷ We repeat conductance measurements for junctions formed from these molecules at regular voltage intervals, and we plot the resulting conductance values in Figures 3a and b (full conductance histograms can be found in the SI). Noting the trends in conductance, we conclude that junctions with **3** exhibit LUMO-dominated transport while **4** results in HOMO-dominated transport. When the voltage exceeds -0.4V, we are unable to form molecular junctions with **3**; for molecule **4**, when the voltage exceeds 0.8V, we find that the conductance begins to decrease with increasing bias.

In the insets of Figures 3a and 3b, we show $T(E)$ as extracted from the bias-dependent conductance measurements for **3** and **4**, respectively. We next quantify energy-level alignment for junctions containing **3** and **4**. Let Γ_L be the electronic coupling between the left electrode and the molecular orbital dominating transport, and Γ_R the coupling to the right electrode. When the junction transmission is dominated by a single level and if the coupling is independent of energy (wide band limit), $T(E)$ can be expressed as a Lorentzian of the form:

$$T(E, \varepsilon, \Gamma) = \frac{\Gamma_L \Gamma_R}{\varepsilon^2 + (\Gamma_L + \Gamma_R)^2 / 4} \quad (4)$$

where ε is the position of dominant conducting orbital relative to the metal Fermi level and we also denote $\Gamma = \Gamma_L = \Gamma_R$. Assuming Eq. (4) holds, we find that the LUMO resonance is located only 0.4 eV from E_F for junctions with molecule **3**; junctions with molecule **4** feature HOMO resonances at -0.7 eV from E_F . This approximation has been shown to be valid for **3**²⁶ based on prior DFT calculations.¹⁸ For **4**, we expect the single-Lorentzian form to be reasonably

accurate given that the high-lying HOMO of **4** is much closer to E_F than the onset of the Au d-states at -1.8eV .⁷

As these peak resonance energies ϵ are well within our accessible source-drain bias range, we should be able to investigate resonant transport through junctions involving molecules **3** and **4**. We therefore measure current-voltage curves for **3** and **4** using a wide bias range. Interestingly, we find that molecule **3** does not form junctions when the applied voltage exceeds the estimated resonance position (0.4V). For molecule **4**, in contrast, we still form well-defined junctions. Yet, the conductance of **4** decreases when the bias is increased beyond the resonance.

To investigate this further, we perform current-voltage measurements for these junctions using a slightly modified break-junction procedure: the tip and substrate are pulled apart for 200 ms at a speed of 16 nm/s, after which the tip-substrate distance is kept constant for 150 ms. During this time, a voltage ramp is applied to the junction. The junction is then pulled apart and broken. Since we are only interested in the behavior of the junction as the bias window approaches a molecular resonance, we only apply a negative voltage ramp for **3** (from 0V to -0.65V) and a positive voltage ramp for **4** (from 0 to 1.6V). We perform thousands of such measurements for each molecule, and analyze these data for junctions that start at a conductance that is representative of a molecular junction for each molecule. Selected traces are then compiled into two-dimensional current vs. voltage histograms in Figure 4a and 4b for **3** and **4**, respectively. We also overlay an averaged current vs voltage trace that is determined by fitting a Gaussian function to each vertical line slice of the two dimensional histogram and plotting its peak value.

From these histograms, it is apparent that junctions with **3** rupture as the bias window is opened beyond the estimated molecular resonance (Figure 4a). A black dashed line is overlaid on the histogram to indicate the position of LUMO estimated from our transmission fit. When the applied bias exceeds this value, it can be seen that the measured current drops to instrumental noise. For molecule **4**, junctions persist even after the bias window exceeds the resonance position (again, indicated by a dashed white line). Indeed, for **4**, we find that the measured current begins to decrease as the bias window has exceeded the molecular resonance (Figure 4b). In either case, as the molecular resonance enters the window between the chemical potentials of the two electrodes, substantial charging of the molecule occurs. For **3**, as the LUMO enters the bias window, it becomes partially occupied, leading to net negative charge on the molecule. For

4, as the HOMO enters the bias window, it becomes partially unoccupied, yielding a net positive charge on the molecule in steady state. Since the orbitals responsible for transport become partially charged, one needs to consider the impact of electron-electron interactions on transport through these junctions. Given the size of these molecules, we estimate that the electrostatic charging energy is larger than the electronic coupling. From our single-Lorentzian fits, we find that $\Gamma \approx 5.3$ meV for **3** and $\Gamma \approx 3.5$ meV for **4** and $\Gamma_L = \Gamma_R = \Gamma$. A simple estimate of the charging energy, U , of a single-molecule can be obtained by approximating the molecule as a metal sphere with a diameter equivalent to the length of the molecule. These U values are on the order of 1eV for **3** and **4**. Interactions with the leads and the electrolytic environment will substantially reduce these values, but U is likely to be larger than Γ .

The above discussion would imply that Coulomb blockade effects should be important, modifying the transmission function across the junction to one that includes the charging energy.⁵ In this case, the transmission function consists of two resonances peaked at e^2/h separated by a charging energy U . We would thus still expect an increase in current with bias voltage as we cross the first resonance and enter the blockaded region. However, this clearly is not what we observe in here. For **3**, we hypothesize that charging the molecule is responsible for rupturing the junction, perhaps because of strongly repulsive electrostatic forces. For **4**, we find that the conductance decreases beyond the resonance peak, which is at odds with the saturation expected from a system with a bias-independent Lorentzian $T(E)$. We thus conclude that for **4**, the shape of the transmission must be changing as the bias increases.

We propose that the decreasing current for **4** is a result of the change of Γ_L and Γ_R in Eq. (4) as a function of bias. Indeed, we expect Γ to change asymmetrically on the two sides of the junction (as we detail below). To understand how the current would be modified by such a change in Γ , we consider an explicit bias dependent coupling: $\Gamma = \Gamma(V)$. For simplicity, we fix ϵ to be -0.7 eV below the substrate Fermi level, as discussed above. (Changes in ϵ with the bias or inclusion of electron-electron interactions will result in small corrections to the model proposed below and can therefore be neglected.) We also assume a completely asymmetric bias drop in this system ($\alpha = 0.5$ as detailed above). We seek $\Gamma_L(V)$ and $\Gamma_R(V)$ such that the integral of the Lorentzian transmission function [Eq. (4)] reproduces the experimental I-V curve. We propose $\Gamma_L(V) = \Gamma_L(0) + c \cdot V$ and $\Gamma_R(V) = \Gamma_R(0) - c \cdot V$, which leads to $\Gamma_L(V) + \Gamma_R(V)$ being independent of bias. We find that $c = 0.003$ reproduces the experimental I-V curve well (Figure 4b). We note

that at zero bias, $\Gamma_L=\Gamma_R=0.005$ eV, consistent with the single-Lorentzian fit we used to determine the location of the resonance. This simple analytic model is physically motivated by the fact that the HOMO polarizes as a function of bias in the junction. Although it does capturing the experimental trends of a decreasing current with increasing bias beyond the resonance, impact of an asymmetric electrolytic environment present in the experiment are not fully accounted for by this simple model.

Conclusion:

We have presented a broadly applicable and experimentally simple method for mapping the transmission function of single-molecule junctions – one of the most fundamental physical characteristics of charge transport. In addition to its simplicity, this method provides access to a large energetic region of the junction transmission function; in principle, this energy range is only be limited by the oxidation and reduction potentials of the solvent in which the measurements are performed. Importantly, this technique provides remarkably fine details on the transmission function, circumventing the need for *a priori* assumptions of functional forms for transmission, as has been done with thermopower measurements, AC measurements, and IV-fitting techniques. Given the control that our method provides over level-alignment in the molecular junction, we are also able to drive charge transport into the resonant regime in junctions containing molecules with favorable initial level alignment. This opens up the exciting possibility to study transport phenomena associated with charged molecular conductors.

Acknowledgments: This work was supported primarily by the National Science Foundation grant DMR-1507440. The computational work was supported by the Molecular Foundry through U.S. Department of Energy, Office of Basic Energy Sciences under Contract No. DE-AC02-05CH11231. Portions of the computation work were performed at NERSC.

References:

1. Muller, C. J.; van Ruitenbeek, J. M.; de Jongh, L. J. *Phys. Rev. Lett.*, **1992**, 69, (1), 140-143.
2. Xu, B. Q.; Tao, N. *J. Science*, **2003**, 301, (5637), 1221-1223.
3. Tao, N. J. *Nat. Nano.*, **2006**, 1, (3), 173-181.
4. Aradhya, S. V.; Venkataraman, L. *Nat. Nano.*, **2013**, 8, (6), 399-410.
5. Datta, S., *Quantum Transport - Atom to Transistor*. Cambridge University Press: 2005.

6. Reddy, P.; Jang, S. Y.; Segalman, R. A.; Majumdar, A. *Science*, **2007**, 315, (5818), 1568-1571.
7. Widawsky, J. R.; Darancet, P.; Neaton, J. B.; Venkataraman, L. *Nano Lett.*, **2012**, 12, (1), 354-358.
8. Kim, T.; Darancet, P.; Widawsky, J. R.; Kotiuga, M.; Quek, S. Y.; Neaton, J. B.; Venkataraman, L. *Nano Lett.*, **2014**, 14, (2), 794-8.
9. Adak, O.; Korytar, R.; Joe, A. Y.; Evers, F.; Venkataraman, L. *Nano Lett.*, **2015**, 15, (6), 3716-3722.
10. Frisenda, R.; Perrin, M. L.; Valkenier, H.; Hummelen, J. C.; van der Zant, H. S. J. *physica status solidi (b)*, **2013**, 250, (11), 2431-2436.
11. Capozzi, B.; Chen, Q.; Darancet, P.; Kotiuga, M.; Buzzeo, M.; Neaton, J. B.; Nuckolls, C.; Venkataraman, L. *Nano Lett.*, **2014**, 14, (3), 1400-1404.
12. Dubi, Y.; Di Ventra, M. *Rev. Mod. Phys.*, **2011**, 83, (1), 131-155.
13. Widawsky, J. R.; Chen, W.; Vazquez, H.; Kim, T.; Breslow, R.; Hybertsen, M. S.; Venkataraman, L. *Nano Lett.*, **2013**, 13, (6), 2889-2894.
14. Liu, Z.-F.; Neaton, J. B. *J. Chem. Phys.*, **2014**, 141, (13), 131104.
15. Darancet, P.; Widawsky, J. R.; Choi, H. J.; Venkataraman, L.; Neaton, J. B. *Nano Lett.*, **2012**, 12, (12), 6250-6254.
16. Perrin, M. L.; Burzurí, E.; van der Zant, H. S. *Chem. Soc. Rev.*, **2015**, 44, (4), 902-919.
17. Pobelov, I. V.; Li, Z. H.; Wandlowski, T. *J. Am. Chem. Soc.*, **2008**, 130, (47), 16045-16054.
18. Capozzi, B.; Xia, J.; Adak, O.; Dell, E. J.; Liu, Z.-F.; Taylor, J. C.; Neaton, J. B.; Campos, L. M.; Venkataraman, L. *Nat. Nano.*, **2015**, 10, (6), 522-527.
19. Venkataraman, L.; Klare, J. E.; Nuckolls, C.; Hybertsen, M. S.; Steigerwald, M. L. *Nature*, **2006**, 442, (7105), 904-907.
20. Nagahara, L. A.; Thundat, T.; Lindsay, S. M. *Rev. Sci. Inst.*, **1989**, 60, (10), 3128-3130.
21. Quek, S. Y.; Kamenetska, M.; Steigerwald, M. L.; Choi, H. J.; Louie, S. G.; Hybertsen, M. S.; Neaton, J. B.; Venkataraman, L. *Nat. Nano.*, **2009**, 4, (4), 230-234.
22. Aradhya, S. V.; Frei, M.; Hybertsen, M. S.; Venkataraman, L. *Nat. Mat.*, **2012**, 11, (10), 872-876.
23. Bard, A. J., L. R. Faulkner, *Electrochemical Methods: Theory and Applications*. Wiley: United States, 2001.
24. Datta, S., *Electronic Transport in Mesoscopic Systems*. Cambridge University Press: 1995.
25. Reuter, M. G.; Solomon, G. C.; Hansen, T.; Seideman, T.; Ratner, M. A. *The Journal of Physical Chemistry Letters*, **2011**, 2, (14), 1667-1671.
26. Dell, E. J.; Capozzi, B.; Xia, J. L.; Venkataraman, L.; Campos, L. M. *Nat. Chem.*, **2015**, 7, (3), 209-214.
27. Huang, H.; Pickup, P. G. *Chemistry of Materials*, **1998**, 10, (8), 2212-2216.

Figures

FIGURE 1

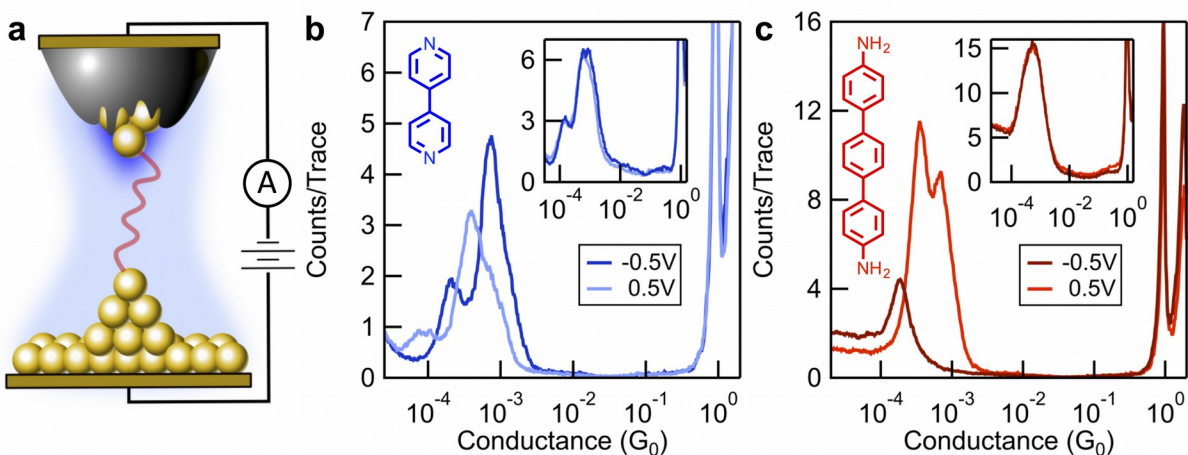


Figure 1: (a) Schematic of molecular junction formed with an insulated STM tip in an ionic environment where the shaded blue region illustrates charged double-layer densities. (b) and (c) Logarithmically binned histograms for 4,4'-bipyridine (1) and 4,4''-p-diaminoterphenyl (2) respectively. Measured in propylene carbonate (PC) at -0.5V and 0.5V (tip relative to substrate) are shown in the main panel while measurements 1-octylbenzene are shown as insets. Histograms for 1 show double peaks corresponding to two different junction conformations in both solvents. Histograms of 2 show a double peak only in PC due to the frequent formation of junctions with two molecules in parallel.

FIGURE 2

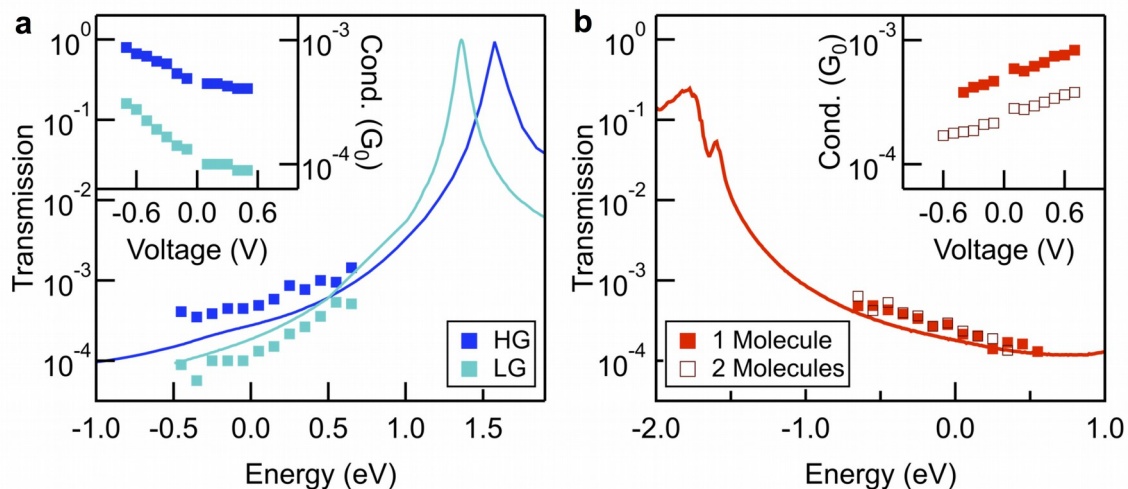


Figure 2: (a) Inset: Peak conductance value versus applied voltage (tip relative to substrate) for the low and high conductance states (LG and HG) for molecule **1**. Main panel: Extracted transmission values for high and low conductance features (HG & LG, markers) for **1** along with DFT+ Σ calculated transmission functions (adapted from reference 8) for the two binding geometries. (b) Peak conductance value versus applied voltage for molecule **2**. Main panel: Extracted transmission values for one- and two-molecule junctions containing **2** along with DFT+ Σ calculated transmission function adapted from reference 8.

Figure 3

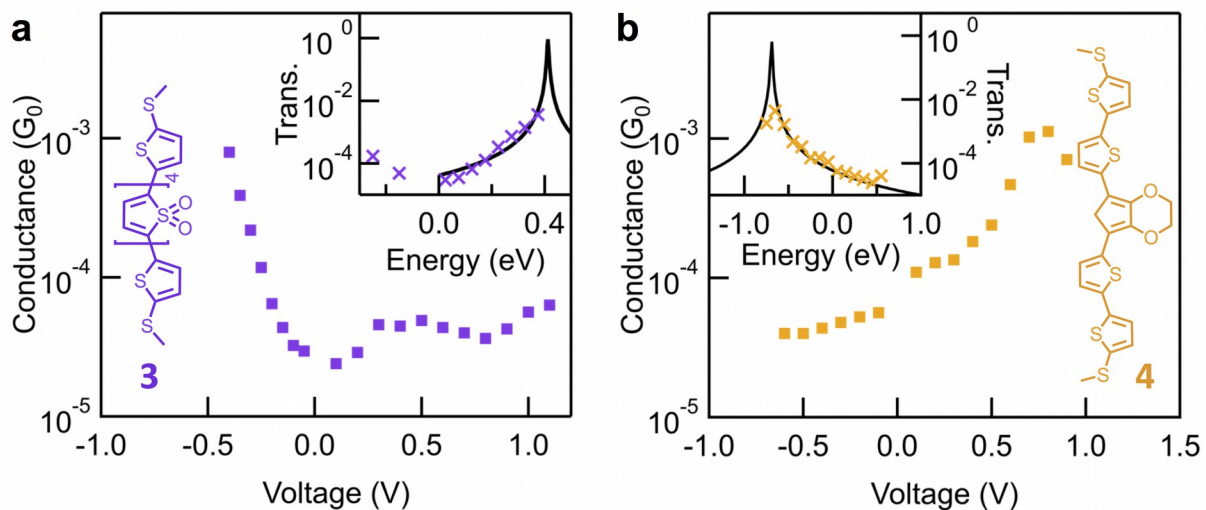


Figure 3: Main panel: Peak conductance value versus applied voltage (tip relative to substrate) with molecular structure shown as an inset for (a) Molecule 3 and (b) Molecule 4. Inset: Extracted transmission values and fit to a single Lorentzian model. Note that only the positive energy values have been fit with the Lorentzian for molecule 3.

FIGURE 4

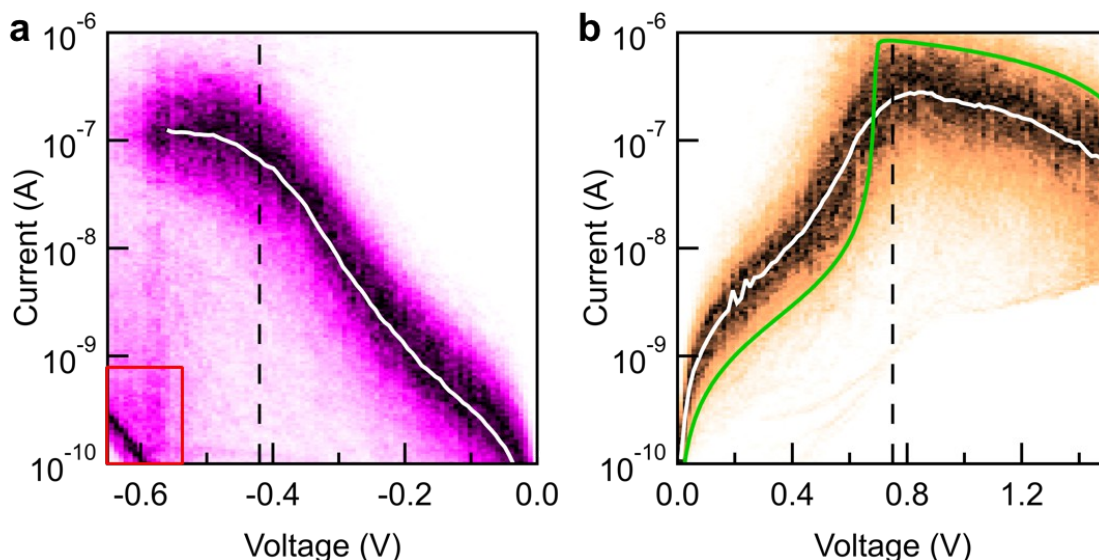


Figure 4: (a) Two-dimensional current-voltage (I-V) histogram constructed from 1574 individual IV curves of molecule **3**. The dashed black line indicates the position of LUMO from conductance versus voltage measurements. It can be seen that molecular junctions rupture frequently beyond this point. The red boxed area in the lower left hand corner shows background current present in junctions where the molecule-metal bond has ruptured. (b) Two-dimensional I-V histogram constructed from 1147 I-V curves of molecule **4**. The dashed black line again indicates the position of the molecular resonance, but in contrast to what is seen with molecule **3**, the junction persists when the applied voltage exceeds the molecular resonance position, and current is seen to now decrease with increasingly positive voltage. White overlay is the average I-V curves and green overlay is the model IV curve obtained by assuming that the coupling to the electrodes becomes asymmetric with applied bias.